High-Fat Diet–Induced DeSUMOylation of E4BP4 Promotes Lipid Droplet Biogenesis and Liver Steatosis in Mice

Sujuan Wang,[1,2] Meichan Yang,[3] Pei Li,[4] Julian Sit,[1] Audrey Wong,[1] Kyle Rodrigues,[1] Daniel Lank,[1,5] Deqiang Zhang,[1] Kezhong Zhang,[6] Lei Yin,[1] and Xin Tong[1]

Diabetes 2023;72:348–361 | https://doi.org/10.2337/db22-0332

Dysregulated lipid droplet accumulation has been identified as one of the main contributors to liver steatosis during nonalcoholic fatty liver disease (NAFLD). However, the underlying molecular mechanisms for excessive lipid droplet formation in the liver remain largely unknown. In the current study, hepatic E4 promoter–binding protein 4 (E4BP4) plays a critical role in promoting lipid droplet formation and liver steatosis in a high-fat diet (HFD)–induced NAFLD mouse model. Hepatic *E4bp4* deficiency (*E4bp4-LKO*) protects mice from HFD-induced liver steatosis independently of obesity and insulin resistance. Our microarray study showed a markedly reduced expression of lipid droplet binding genes, such as *Fsp27*, in the liver of *E4bp4-LKO* mice. E4BP4 is both necessary and sufficient to activate *Fsp27* expression and lipid droplet formation in primary mouse hepatocytes. Overexpression of *Fsp27* increased lipid droplets and triglycerides in *E4bp4-LKO* primary mouse hepatocytes and restored hepatic steatosis in HFD-fed *E4bp4-LKO* mice. Mechanistically, E4BP4 enhances the transactivation of *Fsp27* by CREBH in hepatocytes. Furthermore, E4BP4 is modified by SUMOylation, and HFD feeding induces deSUMOylation of hepatic E4BP4. SUMOylation of five lysine residues of E4BP4 is critical for the downregulation of *Fsp27* and lipid droplets by cAMP signaling in hepatocytes. Taken together, this study revealed that E4BP4 drives liver steatosis in HFD-fed mice through its regulation of lipid droplet binding proteins. Our study also highlights the critical role of deSUMOylation of hepatic E4BP4 in promoting NAFLD.

As the most common chronic liver disease, nonalcoholic fatty liver disease (NAFLD) affects approximately two-thirds of obese individuals and is strongly associated with type 2 diabetes (1,2). The early stage of NAFLD is simple liver steatosis, defined as accumulation of hepatic triglycerides (TGs) >5% of total liver weight (3,4). Although simple liver steatosis is considered largely benign, excessive lipid accumulation may sensitize hepatocytes to stress-induced injury and promote the progression of NAFLD toward nonalcoholic steatohepatitis and cirrhosis (5,6). The excess of lipids found during liver steatosis are primarily neutral lipids stored in organelles called lipid droplets (LDs) in hepatocytes (7,8). The biogenesis of LDs is very dynamic and regulated at both transcriptional and posttranslational levels (7,9). It has been shown that abnormalities in LD biology contribute to fatty liver disease (7,10–12). However, detailed molecular mechanisms underlying the impairment of LD metabolism are largely unclear.

Several proteins, particularly cell death–inducing DNA fragmentation factor α-like effector (CIDE) proteins, were found to regulate LD biogenesis (11,13,14). Both CIDEA and CIDEC (also called FSP27 in mice) are upregulated in obese mice and associated with increased TG storage in the liver (7,14,15). Murine models of hepatic steatosis demonstrated a significant increase in levels of FSP27 in the liver (16–18). The liver of obese humans was revealed to express high levels of FSP27, which tended to decrease after significant weight loss with bariatric surgery (19). Functionally, forced expression of FSP27 in hepatocytes in vitro or in vivo led to increased LD and TG accumulation (18,20).

[1]Department of Molecular and Integrative Physiology, University of Michigan Medical School, Ann Arbor, MI
[2]Department of Infectious Diseases, The Second Xiangya Hospital, Central South University, Changsha, Hunan Province, People's Republic of China
[3]Department of Radiology, Guangdong Provincial People's Hospital, Guangdong Academy of Medical Sciences, Guangzhou, Guangdong Province, People's Republic of China
[4]Center for Advanced Biotechnology and Medicine, Rutgers University, Piscataway, NJ
[5]Department of Pharmacology, University of Virginia, Charlottesville, VA
[6]Center for Molecular Medicine and Genetics, Wayne State University School of Medicine, Detroit, MI

Corresponding authors: Lei Yin, leiyin@umich.edu, and Xin Tong, xintong@umich.edu

Received 6 April 2022 and accepted 6 December 2022

This article contains supplementary material online at https://doi.org/10.2337/figshare.21691973.

S.W. and M.Y. contributed equally to this work.

Depletion of hepatic *Fsp27* with antisense oligo against *Fsp27* ameliorated diet-induced steatohepatitis (21–23). Hepatocyte-specific deletion of *Fsp27* was reported to reduce liver TGs and injury in mice with alcoholic steatohepatitis (18). Collectively, these studies have indicated that elevated levels of FSP27 in the liver could drive liver steatosis in response to overnutrition or obesity. Thus, suppression of FSP27 expression and function might be a viable approach to treating NAFLD.

Transcriptional regulation has been implicated as the major regulatory pathway for controlling the expression of FSP27 in livers (13,14). So far, several transcription factors have been identified to directly regulate the transcription of *Fsp27* within hepatocytes in response to fasting or diets, including peroxisome proliferator–activated receptor-α (PPAR-α), PPAR-γ, liver X receptor-α, hepatocyte nuclear factor-α, and CREB3L3 (also known as CREBH) (16,20,22,24,25). PPAR-γ was found to promote liver *Fsp27* expression in *ob/ob* mice (17), whereas CREBH, a liver-enriched and stress-inducible transcription factor, directly binds to the promoter of *Fsp27* and activates its gene expression (20). Enforced expression of CREBH elevates FSP27 levels and promotes the enlargement of LDs and TG accumulation in mouse liver. However, much less is known about transcriptional mechanisms that account for the induction of *Fsp27* in liver of NAFLD/nonalcoholic steatohepatitis. Moreover, the signaling pathways that suppress *Fsp27* expression in response to overnutrition remain largely unknown.

E4 promoter–binding protein 4 (E4BP4) is a basic leucine zipper transcription factor that has been known for its role in immunomodulation, circadian rhythms, and de novo lipogenesis (26–28). Overexpression of hepatic E4BP4 has been shown to increase gluconeogenesis and induce insulin resistance in both the liver and muscle (29). We previously reported that hepatic E4BP4 is potently induced by endoplasmic reticulum (ER) stress signals. *E4bp4* deficiency reduces accumulation of LDs in hepatocytes following ER stress stimulation (30). Hepatocyte *E4bp4* deficiency also reduces liver steatosis in mice fed a high-fat, low–L-methionine, and choline-deficient diet. Although E4BP4 may impact lipid metabolism in multiple ways within hepatocytes, it remains unclear whether E4BP4 directly regulates LD biogenesis by controlling the expression of LD binding proteins. Intriguingly, E4BP4 was found to interact with CREBH and contribute to CREBH-mediated gene regulation in mouse liver (31). Yet, no study has been reported to link E4BP4 and the expression of *Fsp27* during the pathogenesis of high-fat diet (HFD)–induced liver steatosis.

Protein SUMOylation is an important posttranslational modification that regulates protein turnover, protein-protein interaction, signal transduction, chromatin modifications, and transcription repression (32,33). Recent studies highlighted that SUMOylation of transcriptional factors plays a crucial role in maintaining metabolic homeostasis. It was reported that a SUMOylation-defective mutant of liver receptor homolog 1 enhances SREBP-1 processing and promotes de novo lipogenesis, leading to fatty liver disease (34). In a global SUMOylation analysis, E4BP4 was identified as a putative SUMOylation target (35). Subsequently, E4BP4 was shown to be modified by SUMOylation and identified five specific lysine residues targeted for SUMOylation (36). However, almost nothing is known about the biological actions of E4BP4 SUMOylation in LD formation and lipid accumulation in hepatocytes and during the pathogenesis of fatty liver disease. In this study, we present both in vivo and in vitro evidence supporting the role of hepatic E4BP4 and its SUMOylation during LD expansion in hepatocytes and liver steatosis in response to HFD feeding.

RESEARCH DESIGN AND METHODS

Animals and Treatment

All animal experiments were approved by and performed in accordance with guidelines of the institutional animal care and use committee at the University of Michigan Medical School. Liver-specific *E4bp4* knockout (*E4bp4-LKO*) mice were generated as described previously (30). Eight-week-old *E4bp4*$^{flox/flox}$ and *E4bp4-LKO* mice were challenged with an HFD (45% kcal from fat) for 12 weeks; body weight was recorded weekly. For the FSP27 overexpression experiment, 8-week-old male mice were fed an HFD for 2 weeks. Ad-GFP or Ad-Fsp27 adenovirus was injected via tail vein at a dose of 1.5×10^{11} viral particles/mouse. HFD continued for an additional 10 days prior to liver harvesting for metabolic assays.

Cell Culture and Reagents

Hepa-1c1c cells and Huh-7 cells were purchased from ATCC and maintained according to manufacturer instructions. Isolation of primary mouse hepatocytes (PMHs) was performed by the collagenase perfusion method via inferior vena cava. The reagents used for cell treatment, including norepinephrine forskolin, rapamycin, and AICAR, were all from Cayman Chemical.

BODIPY Staining

E4bp4-LKO PMHs were seeded at the density of 8×10^4 cells/well in a 12-well plate. Ad-LacZ control, Ad-E4bp4, or Ad-Fsp27 adenovirus was applied 2 h after seeding. After being switched to serum-free DMEM (Gibco) the next day, the cells were incubated with 300 μmol/L oleic acid overnight prior to BODIPY (D3922, 493/503, 2 μmol/L; Invitrogen) staining following the protocol described by Qiu and Simon (37). For Huh-7 cells, cells were first transduced with Ad-E4bp4-wild type (WT) or Ad-E4bp4-5KR. Twenty-four hours later, cell culture medium was changed to serum-free minimum essential medium (Gibco), and cells were treated with BSA or palmitic acid (300 μmol/L, dissolved in 0.1 mol/L NaOH at 70°C and conjugated with 10% free fat acid–free BSA in PBS) plus oleic acid (600 μmol/L) for 6 h. Cells were washed with serum-free minimum essential medium once and treated with forskolin at 2.5 μmol/L and 5 μmol/L for 16 h before BODIPY staining.

Liver Histology Analysis

After fixation in 10% formalin at room temperature overnight, mouse liver samples were sent to the Rogel Cancer Center Tissue and Molecular Pathology Shared Resource Core at the University of Michigan Medical School for paraffin embedding and hematoxylin-eosin (H-E) staining.

Protein Extraction and Immunoblotting

For whole-cell lysate preparation, PMHs were washed once in 1× PBS buffer and lysed in radioimmunoprecipitation assay (RIPA) buffer supplemented with 1× protease inhibitor (Roche Applied Science). Liver tissues were weighed and homogenized in RIPA buffer (8 μL/mg tissue weight).

For cytosolic and nuclear protein preparation, liver tissues were weighted, and hypotonic buffer (8 μL/mg tissue weight) was added. Cytosolic protein was collected in the supernatant by using a Dounce homogenizer followed by full-speed centrifugation. The pellet was washed once with hypotonic buffer and resuspended in RIPA buffer (4 μL/mg tissue weight) to obtain the nuclear fraction. After protein lysates were precleared at maximal speed at 4°C in a microfuge, the protein concentration of each supernatant was measured using Bio-Rad Protein Assay Dye. Equal amounts of protein samples were separated using 9% SDS-PAGE and transferred to nitrocellulose membrane (Bio-Rad). The membranes were incubated with primary antibodies at 4°C overnight. Horseradish peroxidase–conjugated secondary antibodies against mouse, rabbit, or goat IgG and homemade enhanced chemiluminescence substrate were used for detecting chemiluminescence on an AlphaImager HD2 (Cell Biosciences).

cDNA Synthesis and Quantitative PCR

Total RNA was extracted with TRIzol (Invitrogen) and chloroform. cDNA was synthesized with M-MLV Reverse Transcriptase and random hexamers (Thermo Fisher Scientific, Surrey, U.K.) and subjected to quantitative PCR (qPCR) using 2× Fast qPCR Mix (ABclonal Science) on an ABI QuantStudio 5 Real-Time PCR System (Applied Biosystems, Foster City, CA). The value of each cDNA was calculated using the ΔΔCt method and normalized to the value of the housekeeping gene controls, including β-actin, Gapdh, or 18S rRNA. The data were plotted as fold change.

Serum and Liver Metabolite Measurement

Serum cholesterol, TGs, and ALT were measured using commercial kits (A7510, A7525, and T7532; Pointe Scientific) according to the manufacturer's instructions. For liver cholesterol and TG content, liver tissues were homogenized for total lipid extraction according to Bligh and Dyer (38). Total lipids were resuspended in 400 μL ethanol and incubated at 55°C for 10 min.

Plasmids and Adenoviruses

A 1.7-kb Fsp27 promoter containing the CREBH responsive element was amplified with primers and ligated with the pGl4 plasmid, which was double digested by *Kpn*I and *Xho*I, to generate the Fsp27 luciferase reporter construct. The mouse Fsp27 coding sequence was first cloned into pDONR/Zeo vector via Gateway BP recombination and then transferred into pAdCMV-DEST plasmid via Gateway LR recombination. All the adenoviruses were generated after transfection of 293AD cells and concentrated by ultracentrifuge in CsCl gradient and purified by Vivaspin 20 concentrators. Ad-shCrebh with the mouse Crebh-targeting sequence of GAGCAGAAAGTTCTACTAAAT was a gift of K.Z.

Transfection and Luciferase Assay

A total of 2×10^5 Hepa1 cells/well were seeded in 24-well plates. Transfection was performed with Opti-MEM (2021431; Gibco) and polyethylenimine. The cells were cotransfected with active Crebh plasmid, E4bp4 plasmid, and Fsp27 luciferase reporter construct along with β-galactosidase (β-gal) plasmid. Twenty-four hours later, luciferase activity was measured with luciferin (103404-75-7; Gold Biotechnology) on a BioTek Synergy 2 microplate reader and normalized by β-gal assay.

Affymetrix Microarray Analysis

Total RNA was extracted from the liver of HFD-fed *E4bp4*$^{flox/flox}$ (n = 4) and *E4bp4-LKO* mice (n = 4). Equal amounts of RNA from the livers of mice of the same genotype were pooled and analyzed at the University of Michigan Medical School Advanced Genomic Core for Affymetrix microarray analysis. Gene expression levels were shown as expression values of $\log_2$-transformed data generated via robust multiarray averages (39). The heat map was generated using the pheatmap R package to compare gene expression levels between HFD-fed *E4bp4*$^{flox/flox}$ and *E4bp4-LKO* mice. The Kyoto Encyclopedia of Genes and Genomes (KEGG) pathway analysis was performed by using the Database for Annotation, Visualization and Integrated Discovery and visualized using the ggplot2 R package.

Coomassie Blue Staining and Mass Spectrometry

A total of 1×10^8 293AD cells was transduced with Ad-GFP or Ad-Flag-E4bp4 for 16 h prior to whole-cell lysate preparation. Protein samples were separated using 9% SDS-PAGE. The gel was stained with Coomassie blue dye for 30 min and destained overnight. The bands showed up only in the Ad-Flag-E4bp4 group and were cut out for mass spectrometry at the Proteomics Resource Facility, Department of Pathology, University of Michigan Medical School.

Statistical Analysis

Statistical analysis was performed using GraphPad Prism 9.3 software. For comparison between two groups, statistical significance was determined by the unpaired two-tailed Student t test. To compare multiple groups, one-way ANOVA with post hoc Tukey test was used in studies with one independent variable, whereas two-way ANOVA with post hoc Tukey test was used for studies with two independent variables. All results are presented as mean ± SEM. Differences were considered statistically significant at $P < 0.05$.

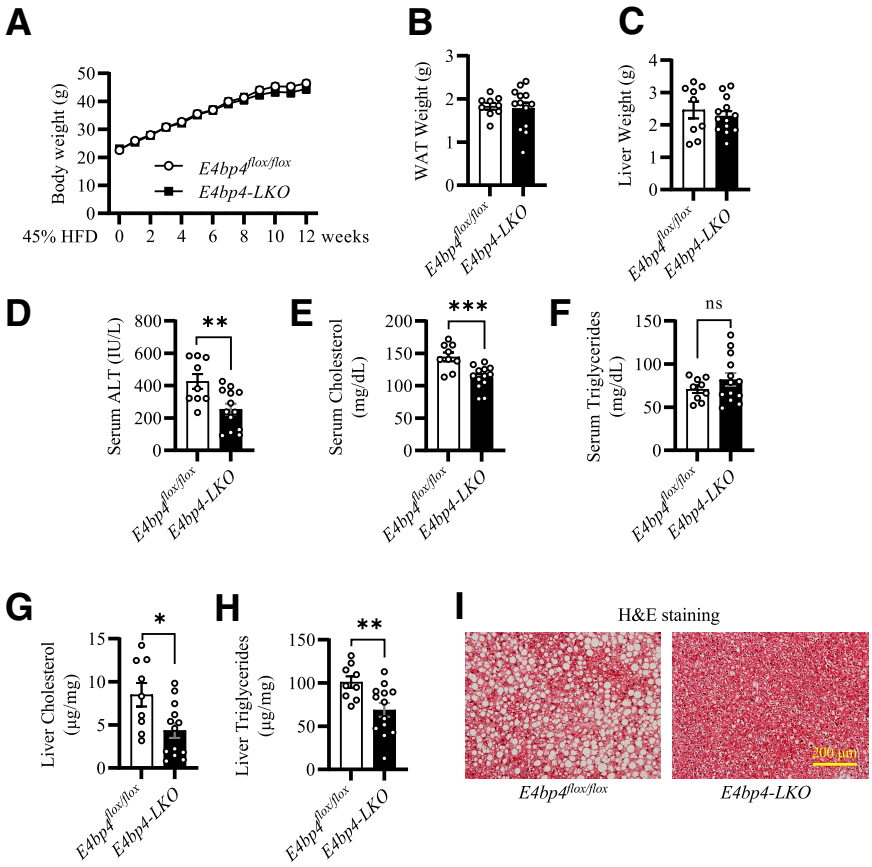

Figure 1—Loss of hepatic *E4bp4* protects mice against HFD-induced liver steatosis. Both 8-week-old *E4bp4* $^{flox/flox}$ male littermates ($n = 9$) and *E4bp4* $^{flox/flox}$ Alb-Cre(+) (*E4bp4-LKO*) male mice ($n = 13$) were fed a 45% HFD for 12 weeks. *A*: Weekly body weight. *B* and *C*: Weight of inguinal white adipose tissue (WAT) and liver. *D*: Serum ALT assay to assess liver injury. *E* and *F*: Serum cholesterol and TG levels. *G* and *H*: Liver cholesterol and TG levels. *I*: Liver H-E staining. *$P < 0.05$, **$P < 0.01$, ***$P < 0.001$.

Data and Resource Availability

All the data and critical resources supporting our findings, as well as methods and conclusions, are available from the corresponding authors upon request. The original Affymetrix microarray data are available in the National Center for Biotechnology Information Gene Expression Omnibus database (GSE 200528).

RESULTS

Hepatic *E4bp4* Deficiency Protects Mice Against HFD-Induced Liver Steatosis

Given the role of E4BP4 in promoting lipogenesis and enhancing lipid accumulation upon ER stress (26,28,30), we hypothesized that hepatic *E4bp4* deficiency may suppress the development of liver steatosis following HFD feeding. To test this hypothesis, both *E4bp4* $^{flox/flox}$ and *E4BP4-LKO* mice were subjected to 12-week HFD feeding. Through the whole feeding period, no differences were observed between *E4BP4-LKO* and *E4bp4* $^{flox/flox}$ mice in body weight, weight of white adipose tissue, and weight of liver (Fig. 1*A*–*C*). Insulin tolerance test after 5 weeks of HFD and glucose tolerance test after 8 weeks of HFD showed no differences between *E4BP4-LKO* and *E4bp4* $^{flox/flox}$ mice (Supplementary Fig. 1*A* and *B*). In addition, overnight fasting glucose was only slightly lower in *E4BP4-LKO* mice, without statistical significance. The expression levels of the key gluconeogenic genes were comparable between the two groups (Supplementary Fig. 1*C* and *D*). These findings indicate that hepatocyte E4BP4 is largely dispensable for body weight gain and glucose metabolism in mice following HFD feeding.

However, we observed a >40% reduction in serum ALT, a serum marker for liver injury (Fig. 1*D*), 20% reduction in serum cholesterol (Fig. 1*E*), and no change in serum TGs in HFD-fed *E4bp4-LKO* mice (Fig. 1*F*). Liver tissues from *E4bp4-LKO* mice contained significantly less TG and cholesterol (Fig. 1*G* and *H*). Further H-E staining also showed greatly reduced lipid accumulation within *E4bp4-LKO* liver (Fig. 1*I*). Liver steatosis at the late stage of NAFLD is associated with increased immune cell infiltration and hepatic stellate cell activation (1,5). By RT-qPCR, a downward trend of fibrosis markers was observed in the liver of *E4bp4-LKO* mice (*Col1a1* and *Col1a2*) (Supplementary Fig. 2*A*). The expression of inflammatory markers was not significantly altered (Supplementary Fig. 2*B*). In summary, hepatic *E4bp4* deficiency protects mice against HFD-induced liver steatosis and liver injury

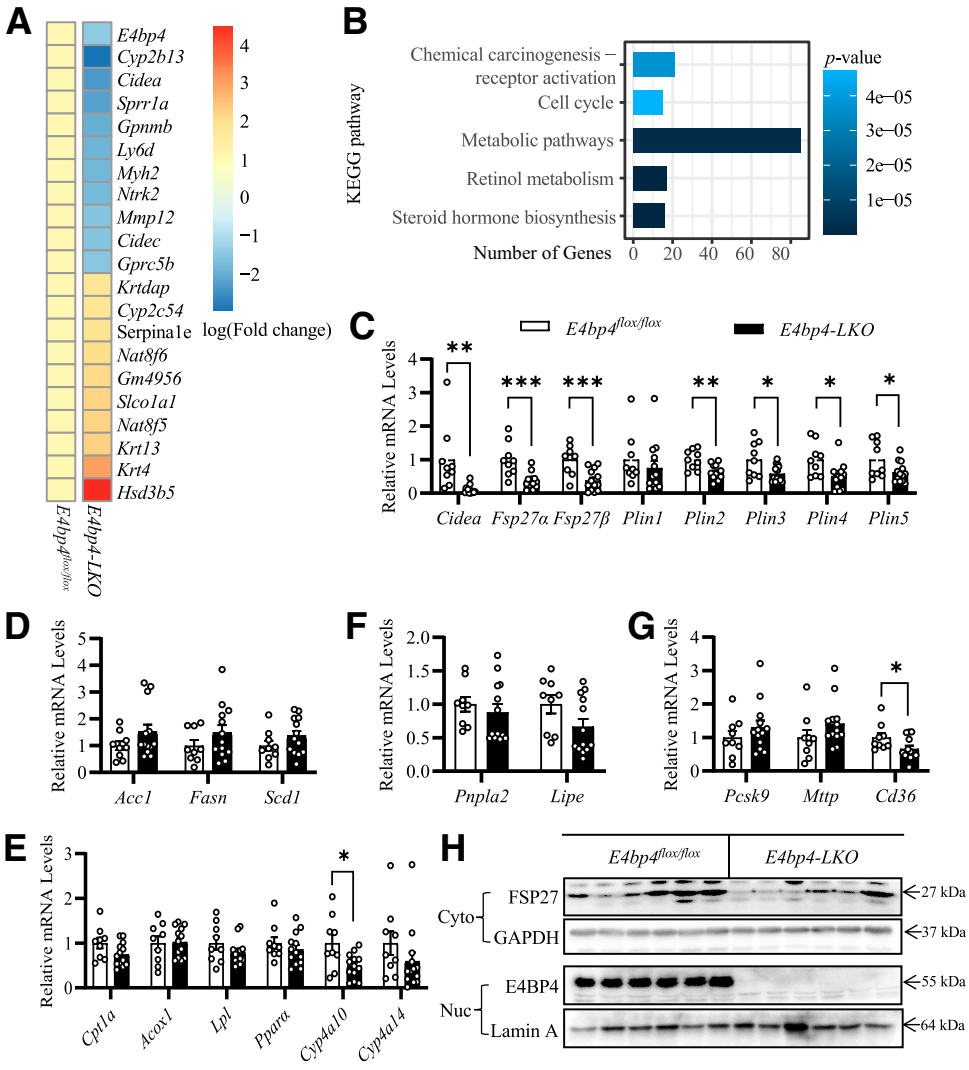

Figure 2—Identification of *Fsp27* as a major downstream target of E4BP4 in the liver of HFD-fed mice. Affymetrix microarray was performed with RNA samples pooled from the livers of HFD-fed *E4bp4*$^{flox/flox}$ male mice (n = 4) vs. *E4bp4-LKO* male mice (n = 4). *A*: Heat map of the top 10 upregulated and downregulated genes (expression values of *E4bp4*$^{flox/flox}$ control mouse livers set at 1). *B*: The top five pathways of KEGG pathway analysis using differentially expressed genes. *C*: The same group of mouse livers were also used for RT-qPCR to assess the expression levels of LD binding genes. *D*–*G*: De novo lipogenic genes, fatty acid oxidation genes, lipolysis genes, and lipid uptake genes. *H*: Immunoblotting to measure the cytosolic (Cyto) FSP27 and nuclear (Nuc) E4BP4 (quantified after normalization in Supplementary Fig. 9). The abundance of Cyto FSP27 was quantified after normalization by GAPDH. *$P < 0.05$, **$P < 0.01$, ***$P < 0.001$.

without affecting adiposity, glucose metabolism, and insulin sensitivity. Altogether, these findings are consistent with our previous report on high-fat, low–L-methionine, and choline-deficient–fed *E4bp4-LKO* mice (30).

Downregulation of LD Binding Proteins in the Liver of *E4bp4-LKO* Mice

To identify downstream pathways regulated by E4BP4 during HFD feeding, we performed a microarray analysis with liver samples from both *E4bp4*$^{flox/flox}$ and *E4BP4-LKO* mice on a 12-week HFD. The microarray heat map highlighted the top 10 upregulated and downregulated genes (>1.5 fold change) (Fig. 2*A*). Among these downregulated genes, *Cidea* and *Cidec* are two classical LD binding proteins (11), whereas *Gpnmb* and *Mmp12* are shown to be involved in liver fibrosis (40,41). As for the upregulated genes, *Cyp2c54* was found to be primarily expressed in the liver, and its function is related to fatty acid oxidation (42). As a solute carrier anion transporter responsible for transporting bile acids into hepatocytes, *Slco1a1* (also called *Oatp1*) expression level was markedly suppressed in the mouse liver following a methionine-choline–deficient diet (43). *Serpina1e* was recently found to be involved in hepatic gluconeogenesis (44). The KEGG pathway analysis showed that metabolic pathways are the most significantly affected by the loss of *E4bp4* in the liver of *E4bp4-LKO* mice (Fig. 2*B*), consistent with the profile of genes observed in microarray analysis.

Next, RT-qPCR analysis was performed to verify the microarray data. Several major LD binding proteins, including *Cidea*, *Fsp27*, and *Plin 2*, *3*, *4*, and *5* were indeed potently

downregulated in the *E4bp4-LKO* liver (Fig. 2*C*). In contrast, no major changes in lipogenic pathway (*Fasn*, *Scd1*, and *Acc1*), fatty acid oxidation (*Cpt1a*, *Acox1*, and *Ehhadh*), and lipolysis (*Pnpla2* and *Lipe*) pathways were detected (Fig. 2*D*–*F*). CD36, a fatty acid translocase, was significantly downregulated in the liver of *E4BP4-LKO* mice (Fig. 2*G*). This is interesting since hepatocyte-specific disruption of CD36 attenuates liver steatosis upon HFD feeding in mice (28,45). The RT-qPCR data showed no differences in genes involved in hepatic cholesterol metabolism between *E4bp4*$^{flox/flox}$ and *E4bp4-LKO* mice (Supplementary Fig. 3). Meanwhile, both E4BP4 and FSP27 protein levels in the liver were markedly reduced in *E4bp4-LKO* mice (Fig. 2*H*). Taken together, our results indicate that hepatic *E4bp4* deficiency reduces HFD-induced liver steatosis and liver injury with a concomitant suppression of LD binding and lipid uptake genes.

E4BP4 Promotes LD Formation and *Fsp27* Expression Via CREBH in Hepatocytes

So far, whether E4BP4 can regulate the expression of *Fsp27* in a cell-autonomous manner remains unclear. To address this question, we manipulated E4BP4 expression in *E4bp4-LKO* PMHs and examined its effect on LD formation and *Fsp27* expression. Loss of *E4bp4* led to a significant decrease of LD numbers in Ad-LacZ–transduced E4bp4-LKO PMHs compared with *E4bp4*$^{flox/flox}$ PMHs. In contrast, adenovirus-mediated overexpression of E4BP4 indeed increased the number of LDs and the expression of the liver-specific *Fsp27β* isoform and *Cidea* in *E4bp4-LKO* PMHs (Fig. 3*A* and *B*). In contrast, acute depletion of *E4bp4* abrogated not only the basal expression of *Fsp27β* but also its induction after stimulation with the saturated fatty acid (palmitate) plus the inflammatory cytokine tumor necrosis factor-α (TNF-α) (Fig. 3*C* and *D*), an in vitro condition mimicking diet-induced nonalcoholic steatohepatitis (46). These results indicate that E4BP4 is both necessary and sufficient to promote the transcription of *Fsp27β* in hepatocytes.

How E4BP4 enhances the transcription of *Fsp27β* intrigued us, since the canonical function of E4BP4 acts as a transcriptional repressor (26,47,48). Furthermore, a genome-wide chromatin immunoprecipitation assay with anti-E4BP4 did not reveal direct binding of E4BP4 to either *Fsp27* or *Cidea* promoter (49). Previously, we reported that E4BP4 stabilizes nuclear SREBP-1c and subsequently enhances SREBP-1c–driven lipogenic gene expression via protein-protein interaction (28). We postulated that E4BP4 might promote the transcription of *Fsp27* indirectly via collaboration with other transcriptional activators of *Fsp27*. We then analyzed the protein levels of several FSP27 regulators (16,20,50) in PMHs transduced with Ad-E4BP4. The immunoblotting results showed that E4BP4 overexpression elevated the abundance of CREBH and SREBP-1c (to a lesser extent) while showing no effects on PPAR-γ (Fig. 3*E*). In contrast, a marked reduction of the nuclear CREBH was observed in the liver of *E4BP4-LKO* mice following HFD feeding (Fig. 3*F*). Consistent with these observations, knockdown of *Crebh* by Ad-shCrebh blocked the induction of *Fsp27β* by E4BP4 overexpression in hepatocytes (Fig. 3*G*). Furthermore, we tested the effects of E4BP4 on the activity of the mouse *Fsp27* promoter, which was reported to contain a binding site for CREBH (20). Compared with active CREBH overexpression, E4BP4 alone had minimal induction of the *Fsp27* promoter–driven luciferase reporter in Hepa1 cells (Fig. 3*H*). However, its overexpression significantly boosted the CREBH-induced transaction of *Fsp27*, supporting that E4BP4 most likely promotes the *Fsp27* transcription via CREBH.

We also examined whether SREBP-1c could be involved in E4BP4-stimulated expression of *Fsp27*. Acute depletion of *Srebp-1c* also tended to reduce the ability of E4BP4 to induce the *Fsp27* expression without reaching statistical significance (Supplementary Fig. 4). In summary, these data suggest a link between E4BP4 and CREBH, pointing to E4BP4 as a critical regulator of *FSP27* expression mainly via CREBH in hepatocytes.

Overexpression of FSP27 in the Liver of *E4BP4-LKO* Mice Restores Liver Steatosis

Next, we investigated to what extent FSP27 mediates the effects of E4BP4 on lipid content and the number of LDs in the liver. For this purpose, an adenovirus expressing the *Fsp27α* isoform (Ad-Fsp27) was generated and used to transduce PMHs along with Ad-LacZ control. Of note, the functional motifs of FSP27α and FSP27β are almost indistinguishable despite tissue-specific expression patterns (18,20). Indeed, compared with Ad-LacZ–transduced *E4bp4-LKO* PMHs, Ad-Fsp27 markedly increased the number of LDs in *E4bp4-LKO* PMHs (Fig. 4*A*). Next, we injected *E4bp4*$^{flox/flox}$ mice with Ad-GFP and *E4bp4-LKO* mice with Ad-GFP control or Ad-Fsp27 after 2 weeks of HFD feeding and then examined liver lipid metabolism 10 days later. By the end of the experiment, we confirmed overexpression of *Fsp27* at both mRNA and protein levels (Fig. 4*B* and *C*). The total liver TG content was increased significantly in the Ad-Fsp27–injected *E4bp4-LKO* mice versus the Ad-GFP–injected *E4bp4-LKO* mice (~2.8-fold, $P < 0.01$) (Fig. 4*D*). The total cholesterol content showed no significant difference among the three groups (Fig. 4*E*). Liver H-E staining revealed that both the size and number of LDs were markedly increased by Ad-Fsp27 in *E4bp4-LKO* mice (Fig. 4*F*). However, no differences were found in terms of serum levels of ALT, TGs, and cholesterol among the three groups of mice (Supplementary Fig. 5*A*–*C*). Thus, both in vitro and in vivo data support that *FSP27* is a downstream effector that links E4BP4 and liver steatosis in response to HFD feeding.

Nutritional Stresses Induce DeSUMOylation of E4BP4 in the Liver and Hepatocytes

So far, we have demonstrated that E4BP4 overexpression stimulates the expression of *Fsp27* in hepatocytes. We

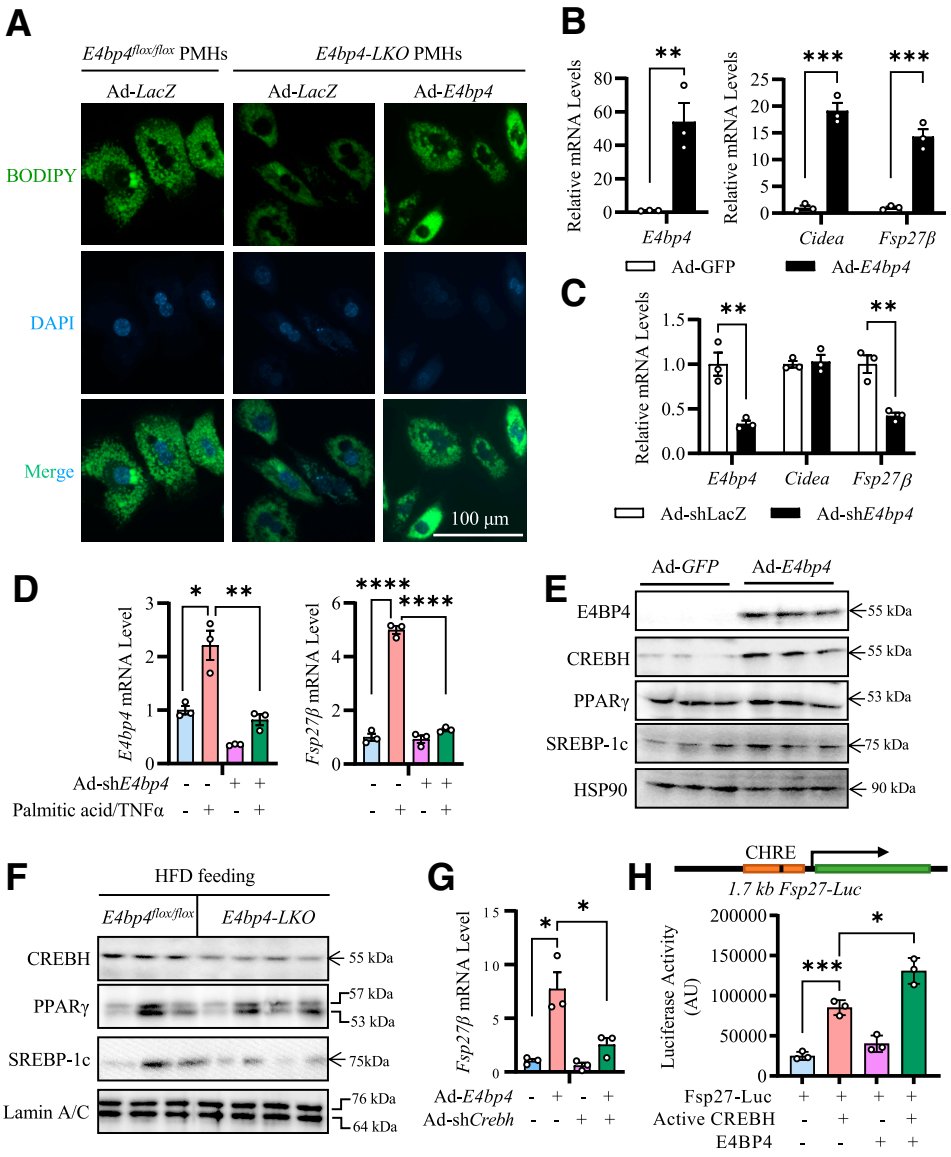

Figure 3—E4BP4 promotes LD formation and *Fsp27* expression via CREBH in hepatocytes. *A*: Induction of LDs in *E4bp4-LKO* PMHs by E4bp4 overexpression. *E4bp4-LKO* PMHs were transduced with Ad-LacZ or Ad-E4bp4, while *E4bp4* $^{flox/flox}$ PMHs were transduced with Ad-LacZ as control before oleic acid (300 μmol/L) treatment overnight and then BODIPY staining for LDs (quantified in Supplementary Fig. 10). *B*: *E4bp4*, *Cidea*, and *Fsp27β* expression levels in *E4bp4-LKO* PMHs following *E4bp4* overexpression. *C*: *E4bp4*, *Cidea*, and *Fsp27β* expression levels in PMHs from *E4bp4* $^{flox/flox}$ mice following *E4bp4* knockdown by Ad-shE4bp4. *D*: Effect of acute depletion of *E4bp4* on *Fsp27β* expression in *E4bp4* $^{flox/flox}$ PMHs with and without palmitic acid (200 μmol/L) plus TNF-α (8 ng/mL) treatment. *E*: Effect of E4BP4 overexpression on lipid metabolism genes in PMHs. The abundance of CREBH was quantified after normalization by HSP90 (Supplementary Fig. 9). *F*: Comparison of the abundance of FSP27 regulators in the liver between *E4bp4* $^{flox/flox}$ and *E4bp4-LKO* mice following HFD feeding. The abundance of CREBH was quantified after normalization by Lamin A/C (quantified in Supplementary Fig. 9). *G*: Effect of *E4bp4* overexpression and *Crebh* knockdown on *Fsp27β* expression level. PMHs were transduced with Ad-E4bp4, Ad-shCrebh, or both before RT-qPCR for *Fsp27β* expression. *H*: Enhancement of CREBH-induced *Fsp27* promoter activity by ectopic expression of *E4bp4* in hepatocytes. Hepa1 cells were transfected with a 1.7-kb *Fsp27* promoter–driven luciferase reporter construct, active *Crebh* expression construct, or *E4bp4* expression construct. Luciferase activity was normalized by β-gal activity. **P* < 0.05, ***P* < 0.01, ****P* < 0.001, *****P* < 0.0001. AU, arbitrary unit; CHRE, CREBH response element.

also showed that such action primarily depends on CREBH. These findings raised an important question of how exactly E4BP4, a transcriptional repressor, activates the expression of *Fsp27*. To test the possibility that E4BP4 could change its transcriptional activity via posttranslational modifications, we transduced PMHs with Ad-Flag-E4bp4 and performed immunoprecipitation with anti-FLAG for proteomic analysis to identify novel interaction proteins and posttranslational modifications of E4BP4. Two distinctive bands were cut out for proteomic analysis of the immunocomplex of E4BP4 (Fig. 5*A*). The top band had a higher molecular weight than that of E4BP4 and was shown to be an E4BP4-dominant protein

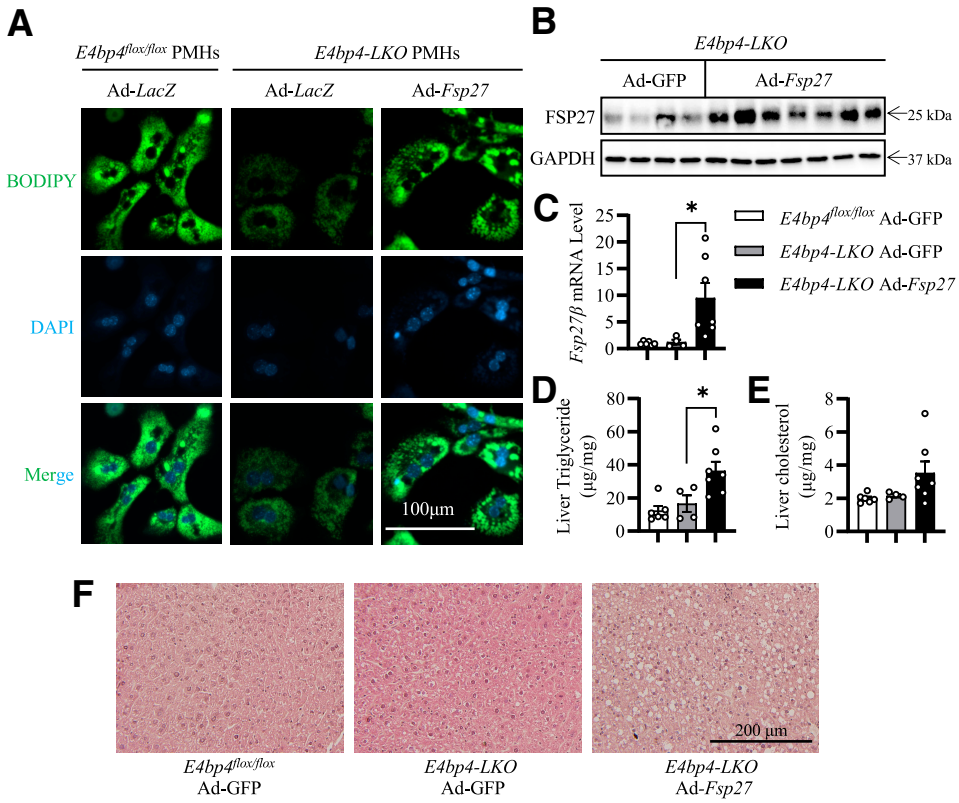

Figure 4—Restoring *Fsp27* in the liver of *E4bp4-LKO* mice rescues liver steatosis after HFD feeding. *E4bp4-LKO* PMHs were transduced with Ad-LacZ or Ad-Fsp27 and then treated with oleic acid (300 μmol/L). Ad-LacZ–transduced *E4bp4* $^{flox/flox}$ PMHs were included as control. *A*: After overnight incubation, PMHs were subjected to BODIPY staining for LDs (quantified in Supplementary Fig. 10). *B–F*: After 2-week HFD feeding, 8-week-old male *E4bp4* $^{flox/flox}$ mice were injected with Ad-GFP control via tail vein, while 8-week-old male *E4bp4-LKO* mice were injected with Ad-GFP control or Ad-Fsp27 virus. Ten days after injection, mouse livers were harvested for immunoblotting (quantified after normalization by GAPDH in Supplementary Fig. 9) (*B*); RT-qPCR for *Fsp27β* expression (*C*), liver TG (*D*), and cholesterol (*E*) levels; and liver H-E staining (*F*). *$P < 0.05$.

complex that contained metastasis associated 1 family member 2 (MTA2), small ubiquitin-like modifier 2 (SUMO2), SUMO3, GATA binding protein 2A (GATA2A), and GATA2B (Fig. 5*B*). The lower band matched the molecular weight of E4BP4 that was identified as the major constituent along with a panel of other transcriptional regulators. Transducin β-1 X-linked (TBL1) and its receptor TBLR1 were reported to function as a transcription cofactor in controlling lipid mobilization in white adipose tissue (51). WD-repeat domain 1 (WDR1) is a major cofactor of the actin depolymerizing factor and accelerates actin disassembly. Mice with *Wdr1* deficiency in cardiomyocytes exhibit cardiac hypertrophy and myocardial fibrosis (52). Histone deacetylase 2 (HDAC2), one of the class I HDAC enzymes, has been shown to have diverse biological function in cellular metabolism and liver diseases (53). Finally, lysing acetyltransferase 8 (KAT), is an important epigenetic regulator for embryonic development and normal chromatin architecture (54). Recently, KAT8 was also found to play a role in liver metabolism and liver injury (55,56). Until now, the interactions between E4BP4 and these epigenetic regulators are novel and unexpected. We suspect that E4BP4 might function differently via interacting with different transcription cofactors or epigenetic regulators.

The proteomic finding that E4BP4 coexists with SUMO2 and SUMO3 peptides in hepatocytes prompted us to postulate that E4BP4 might be modified by SUMOylation in hepatocytes. In fact, E4BP4 was found to be modified by SUMOylation in 293T cells via an unbiased screen (35). The five lysine residues within E4BP4 for SUMOylation were identified in a recent report (36) (Fig. 5*C*). To verify our proteomic finding, we performed an in vitro SUMOylation assay using purified glutathione S-transferase (GST)-E4BP4 and recombinant SUMO enzymes with or without Mg^{2+} plus ATP (Mg-ATP). Indeed, compared with GST alone control, GST-E4BP4 showed distinct bands of SUMO2/3 conjugations in the presence of SUMO enzymes in an Mg-ATP–dependent manner (Fig. 5*D*). Taken together, our data not only confirm that E4BP4 is a direct target of SUMOylation but also demonstrate for the first time that E4BP4 SUMOylation occurs in hepatocytes.

Protein SUMOylation is dynamically regulated by hormonal and nutritional signaling (32). For example, SUMOylation of hepatic bile acid sensor farnesoid X receptor was found to be reduced upon HFD feeding, while its acetylation was elevated in the liver (57). We therefore asked whether hepatic E4BP4 SUMOylation is also regulated

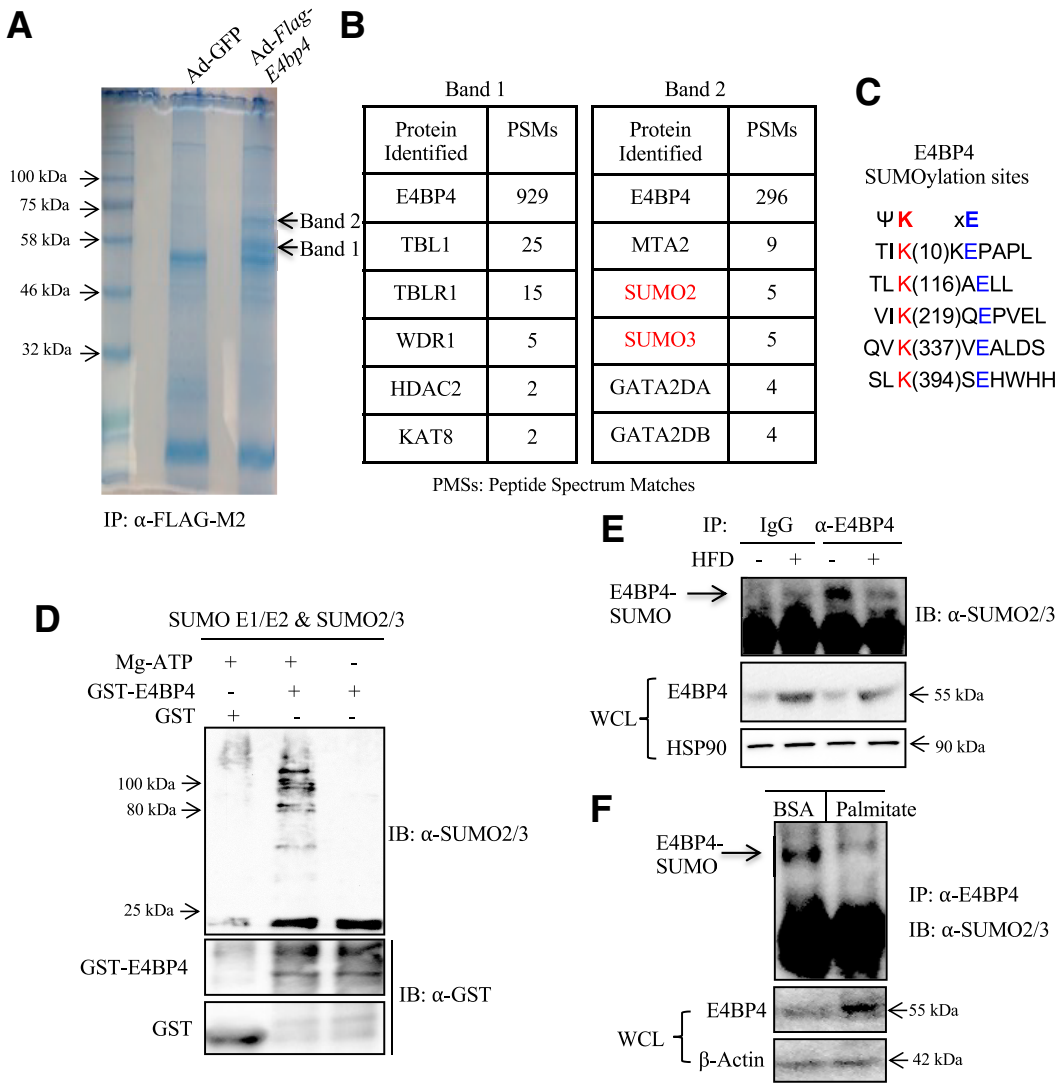

Figure 5—Nutritional stress induces deSUMOylation of E4BP4. *A*: Coomassie blue staining of the E4BP4-FLAG–associated protein bands after immunoprecipitation (IP) with anti-FLAG. PMHs isolated from *E4bp4*$^{flox/flox}$ mice were transduced with Ad-GFP vs. Ad-FLAG-E4bp4 and used for IP with anti-FLAG. The two bands cut out for mass spectrometry are indicated. *B*: Bands identified in the immunocomplex of E4BP4 and their peptide spectrum match (PSM) numbers. *C*: Five lysine residues within E4BP4 protein targeted for SUMOylation. *D*: In vitro E4BP4 SUMOylation assay using purified GST-E4BP4, SUMO2/3, and recombined SUMO enzymes. *E*: In vivo SUMOylation assay with the liver from mice fed regular chow vs. HFD for 10 weeks. *F*: In vitro SUMOylation assay. Hepa1 cells were treated with palmitate at 400 μmol/L overnight before lysis for IP with anti-E4BP4 and immunoblotting (IB) with anti-SUMO. WCL, whole-cell lysate.

by nutritional signaling. We first examined E4BP4 SUMOylation in the liver after HFD feeding. E4BP4 SUMOylation was detected in the liver of regular chow–fed mice but became largely undetectable after 10 weeks of HFD feeding despite elevated hepatic E4BP4 protein (Fig. 5*E*). Next, we addressed whether specific nutritional signals could promote deSUMOylation of E4BP4 within hepatocytes. We chose to test palmitate, the saturated fatty acid known to be associated with liver steatosis, insulin resistance, and ER stress (6). After overnight treatment with palmitate at 400 μmol/L, E4BP4 SUMOylation was markedly reduced, whereas the E4BP4 total protein increased, reminiscent of the pattern in mouse liver after HFD feeding (Fig. 5*F*). Taken together, our data suggest that hepatic E4BP4 exists in both SUMOylated and deSUMOylated states. More importantly, nutritional stress, including HFD feeding and palmitate treatment, can lead to deSUMOylation of E4BP4 in the liver and hepatocytes.

Effects of E4BP4 DeSUMOylation on *Fsp27* Expression and LD Formation in Hepatocytes

To further investigate the biological significance of E4BP4 SUMOylation in regulating hepatic lipid metabolism, we generated adenoviruses to express E4BP4-WT and E4BP4-5KR respectively. Since protein SUMOylation affects both protein stability and activity, we compared the protein stability of E4BP4-WT and E4BP4-5KR mutant in a cycloheximide chase experiment. As shown in Supplementary Fig. 6*A*, both

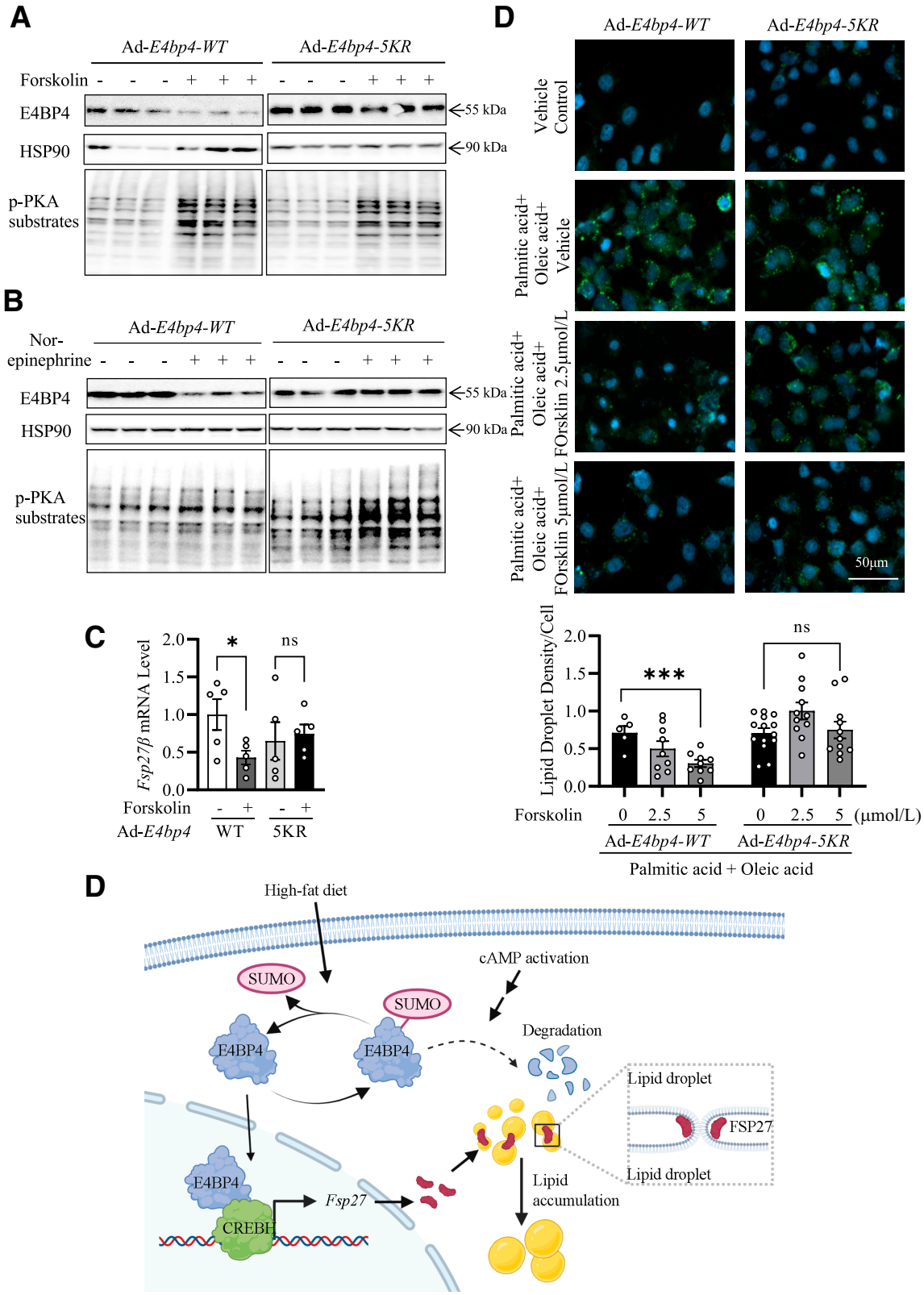

Figure 6—Reduced sensitivity of deSUMOylated E4BP4 to the suppression of *Fsp27* expression and LD formation by cAMP activation in hepatocytes. *A* and *B*: Effect of forskolin and norepinephrine on E4BP4 protein abundance in hepatocytes. Hepa1 cells were transduced with Ad E4BP4-WT or E4BP4-5KR and treated with forskolin at 20 μmol/L or norepinephrine at 5 nmol/L for 6 h prior to Western blot for E4P4 abundance with anti-E4BP4 and PKA activation with anti–p-PKA substrates. The abundance of E4BP4 and p-PKA substrates was quantified after normalization by HSP90 (Supplementary Fig. 9). *C*: Comparison of *Fsp27β* levels in Hepa1 cells overexpressing E4BP4-WT vs. E4BP4-5KR after forskolin treatment. Hepa-1c1c7 cells were transduced with Ad-E4bp4-WT vs. Ad-E4bp4-5KR for

E4BP4-WT and E4BP4-5KR exhibited similar rates of degradation, consistent with a previous report (36). Functionally, both E4BP4-WT and E4BP4-5KR significantly upregulated *Fsp27β* and enhanced the protein abundance of CREBH in PMHs (Supplementary Fig. 6*B* and *C*). Furthermore, we found that both E4BP4-WT and E4BP4-5KR interacted with CREBH in a coimmunoprecipitation assay (Supplementary Fig. 6*D*). Taken together, nonSUMOylatable E4BP4-5KR mutant behaves similarly to E4BP4-WT at basal and nonstimulated conditions.

During fasting, breakdown of LDs and lipolysis are stimulated by signals, including cAMP/cAMP-dependent protein kinase (PKA), AMPK, and inhibition of mammalian target of rapamycin (58–60). We therefore examined whether E4BP4-WT and E4BP4-5KR respond differently to these signaling pathways. Both E4BP4-WT and E4BP4-5KR behaved similarly in the presence and absence of rapamycin or AICAR treatment (Supplementary Fig. 7*A* and *B*). However, in the presence of forskolin, a cAMP/PKA activator, E4BP-WT degraded within 6 h after treatment, significantly faster than E4BP4-5KR (Fig. 6*A*). Given the potent activation of PKA and lipolysis by norepinephrine in hepatocytes (61), we also treated hepatocytes with norepinephrine and observed a similar pattern where norepinephrine stimulated the degradation of E4BP4-WT but not E4BP4-5KR (Fig. 6*B*), supporting that deSUMOylation renders E4BP4 more resistant to protein degradation induced by activation of the cAMP pathway.

To further determine whether forskolin affects E4BP4-dependent *Fsp27* expression in hepatocytes, we transduced Hepa-1c1c7 cells with Ad-E4bp4-WT versus Ad-E4bp4-5KR and treated cells with forskolin. Forskolin potently downregulated *Fsp27β* in Ad-E4bp4-WT–transduced Hepa1 cells. However, the suppression of *Fsp27β* by forskolin was completely lost in Hepa1 cells transduced with Ad-E4bp4-5KR (Fig. 6*C*). Meanwhile, other forskolin-sensitive genes, such as *G6pse* and *Il11*, were not affected by overexpression of E4BP4 (Supplementary Fig. 8*A*) (62). Interestingly, forskolin also reduced CREBH protein in Hepa1 cells transduced with either Ad-GFP or Ad-E4bp4-WT. However, the suppression of *CREBH* by forskolin was completely lost in Hepa1 cells overexpressing E4bp4-5KR (Supplementary Fig. 8*B*), consistent with the unchanged mRNA levels of *Fsp27β* in Ad-E4bp4-5KR–transduced Hepa1 cells (Fig. 6*C*). These observations provide further evidence supporting that deSUMOylation of E4BP4 protects CREBH-dependent Fsp27 expression under the cAMP activation condition.

Finally, we examined LD formation in Huh-7 cells following treatment of forskolin in the presence of overexpression of E4BP4-WT versus E4BP4-5KR. After incubation with a mixture of palmitate and oleate, which was shown to induce LD formation in hepatocytes (63), both E4BP4-WT and E4BP4-5KR–expressing cells accumulated similar numbers of LDs. In E4BP4-WT–expressing Huh-7 cells, forskolin treatment at both 2.5 μmol/L and 5 μmol/L significantly reduced the number of LDs. In contrast, forskolin treatment at 2.5 μmol/L failed to block the increase of LDs in E4BP4-5KR–expressing cells (Fig. 6*D*). However, forskolin at 5 μmol/L still showed a minimal inhibitory effect on LD formation in cells with E4BP4-5KR overexpression, suggesting that there are E4BP4-independent mechanisms for the suppression of LD formation by forskolin. Taken together, our data uncover a novel link between the status of E4BP4 SUMOylation and cAMP activation–mediated suppression of LD biogenesis.

DISCUSSION

In this study, we demonstrated the essential role of E4BP4 in driving hepatic FSP27 through CREBH to expand LDs in response to HFD feeding. Our data highlight that deSUMOylation of E4BP4 blocks the inhibitory effects of cAMP pathway activation on *Fsp27* expression and LD formation in hepatocytes, potentially leading to the development of NAFLD.

Our study is the first to demonstrate that E4BP4 is one of the master regulators of LD binding proteins during NAFLD. There is mounting evidence that LD binding proteins play important roles in regulating LD biogenesis and catabolism (10,12). In our study, we discovered and confirmed the marked downregulation of several major LD binding proteins in the liver of *E4bp4-LKO* mice, including *Cidea*, *Cidec* (*Fsp27* in mice), *Plin2*, *Plin3*, and *Plin4*, and to a lesser degree *Plin1* and *Plin5*. We focused on how hepatic E4BP4 promotes *Fsp27* expression because of the following reasons: *1*) FSP27 is a liver-enriched CIDE-type LD binding protein (20); *2*) upregulation of *Fsp27* by CREBH, PPAR-γ, and SREBP-1c has been linked to LD growth and hepatic steatosis (16,20,50); and *3*) administration of *Fsp27* antisense oligos improves diet-induced steatohepatitis in mice (21,23), suggesting that a tight control of *Fsp27* expression could be a key step to treating fatty liver diseases. Although the exact mechanisms remain to be further defined, we demonstrated that knockdown of *Crebh* abrogates the induction of *Fsp27β* by E4BP4, supporting that E4BP4 promotes the transcription of *Fsp27β* via CREBH. Hepatic CREBH protein has been shown to depend on E4BP4 (31), prompting us to speculate that E4BP4 might promote *Fsp27* transcription by maintaining the CREBH stability.

36 h and then subjected to forskolin (20 μmol/L) for 6 h before RT-qPCR. *D*: Image and quantification of LDs in Huh-7 cells overexpressing E4BP4-WT vs. E4BP4-5KR in response to forskolin treatment. Prior to BODIPY staining for LDs, Huh-7 cells were transduced with either Ad-E4BP4-WT or E4BP4-5KR for 36 h. Cells were then subjected to palmitic acid (300 μmol/L) plus oleic acid (600 μmol/L) for 6 h before treatment with increasing concentrations of forskolin for 16 h. LD density was quantified using ImageJ software and normalized by cell numbers. *E*: Schematic model depicting regulation of LD formation and *Fsp27* expression by E4BP4 via CREBH and deSUMOylation in hepatocytes in response to cAMP activation and HFD feeding. $^*P < 0.05$, $^{***}P < 0.001$.

In this study, we examined the role of protein SUMOylation in regulating E4BP4 action on FSP27 expression. Protein SUMOylation has emerged as a critical modification during cellular responses to various stresses, including hypoxic and oxidative stress, and more recently ER stress (64). It has been reported that XBP1, the key transcription factor regulating ER stress response, is modified by SUMOylation, and SUMOylated XBP1 is more stable than the unmodified XBP1 (65). Moreover, ATF6 protein can be modified by SUMOylation, and its transcriptional activity is suppressed by SUMOylation (66). These findings suggest that the outcomes of SUMOylation are transcription factor specific. We also found that E4BP4 is modified by SUMOylation in a SUMO2/3-dependent manner and that SUMOylation of E4BP4 is sensitive to nutritional status in hepatocytes. We speculate that SUMOylation status of E4BP4 depends on the activity of both SUMO E3 ligases and deSUMOylases within hepatocytes. So far, PIASy, one of the SUMO E3 ligases, has been reported to regulate hepatic lipid metabolism upon fasting signaling (67). In contrast, SENP3, one of the SUMO-specific proteases, was found to act as a key regulator of hepatic lipid metabolism in NAFLD (68). We intend to identify the specific enzymes that control the reversible E4BP4 SUMOylation in future work.

Our data show that SUMOylation does not impact E4BP4 protein degradation or its ability to induce the CREBH-*Fsp27β* axis in hepatocytes under basal conditions. However, our data did reveal that the nonSUMOylatable E4BP4-5KR mutant is resistant to activation of the cAMP pathway, a key signaling pathway in regulating carbohydrate and lipid metabolism in the liver during fasting-feeding cycles and nutritional stress (58,59,69). Accumulated evidence suggests that elevated cAMP signaling confers protection against diet-induced NAFLD in mice, whereas inhibition of cAMP signaling is sufficient to trigger NAFLD (70–72). Our work uncovered that activation of the cAMP pathway by forskolin not only lowers the protein levels of E4BP4-WT but also downregulates the CREBH-*Fsp27β* axis, subsequently reducing LDs within hepatocytes. However, these effects are largely absent in hepatocytes expressing the SUMOylation-defective E4BP4-5KR mutant, supporting a critical role of E4BP4 SUMOylation in mediating the inhibitory effects of cAMP pathway activation on CREBH-FSP27–dependent LD biogenesis. Given the importance of the cAMP pathway in liver physiology and liver disease, it would be of great interest to identify both upstream signaling and downstream effectors of the cAMP pathway in regulating the SUMOylation and stability of E4BP4 in NAFLD.

Funding. This work was supported by National Institutes of Health grant R01 DK121170 (to X.T.). Part of the work was also supported by Michigan Nutrition Obesity Research Center pilot grant P30 DK089503 (to L.Y.) and Michigan Diabetes Research Training Center pilot grant P60 DK020572 (to X.T.). J.S. and A.W. were supported by the Molecular and Integrative Physiology Short Term Educational Program (R25 DK088752).

Duality of Interest. No potential conflicts of interests relevant to this article were reported.

Author Contributions. S.W., M.Y., J.S., K.R., and D.L. performed the RNA extraction from cells/tissues, RT-qPCR, genotyping PCR, and phenotyping of *E4bp4-LKO* mice after HFD feeding. M.Y., J.S., and L.Y. performed the BODIPY and biochemical experiments. M.Y. and D.Z. performed the primary hepatocyte isolation. M.Y. and X.T. generated all the expression vectors and recombinant adenoviruses for the in vitro and in vivo experiments. P.L. performed affinity purification of the E4BP4 protein for mass spectrometry. J.S. performed the in vitro SUMOylation assay. A.W. created the Fsp27 promoter–driven luciferase reporter construct. K.Z. provided the Ad-shCrebh adenovirus. L.Y. provided input on the manuscript. X.T. supervised the project and wrote the manuscript. All authors reviewed and commented on the manuscript. X.T. is the guarantor of this work and, as such, had full access to all the data in the study and takes responsibility for the integrity of the data and the accuracy of the data analysis.

Prior Presentation. Parts of this study were presented in abstract form at the 2022 Federation of American Societies for Experimental Biology Meeting on Lipid Droplets, Asheville, NC, 26–30 June 2022.

References

1. Dewidar B, Kahl S, Pafili K, Roden M. Metabolic liver disease in diabetes - from mechanisms to clinical trials. Metabolism 2020;111S:154299
2. Tilg H, Moschen AR, Roden M. NAFLD and diabetes mellitus. Nat Rev Gastroenterol Hepatol 2017;14:32–42
3. Friedman SL, Neuschwander-Tetri BA, Rinella M, Sanyal AJ. Mechanisms of NAFLD development and therapeutic strategies. Nat Med 2018;24:908–922
4. Brunt EM, Kleiner DE, Carpenter DH, et al.; American Association for the Study of Liver Diseases NASH Task Force. NAFLD: reporting histologic findings in clinical practice. Hepatology 2021;73:2028–2038
5. Buzzetti E, Pinzani M, Tsochatzis EA. The multiple-hit pathogenesis of non-alcoholic fatty liver disease (NAFLD). Metabolism 2016;65:1038–1048
6. Marra F, Svegliati-Baroni G. Lipotoxicity and the gut-liver axis in NASH pathogenesis. J Hepatol 2018;68:280–295
7. Mashek DG, Khan SA, Sathyanarayan A, Ploeger JM, Franklin MP. Hepatic lipid droplet biology: getting to the root of fatty liver. Hepatology 2015;62:964–967
8. Olzmann JA, Carvalho P. Dynamics and functions of lipid droplets. Nat Rev Mol Cell Biol 2019;20:137–155
9. Seebacher F, Zeigerer A, Kory N, Krahmer N. Hepatic lipid droplet homeostasis and fatty liver disease. Semin Cell Dev Biol 2020;108:72–81
10. Carr RM, Ahima RS. Pathophysiology of lipid droplet proteins in liver diseases. Exp Cell Res 2016;340:187–192
11. Chen FJ, Yin Y, Chua BT, Li P. CIDE family proteins control lipid homeostasis and the development of metabolic diseases. Traffic 2020;21:94–105
12. Gluchowski NL, Becuwe M, Walther TC, Farese RV Jr. Lipid droplets and liver disease: from basic biology to clinical implications. Nat Rev Gastroenterol Hepatol 2017;14:343–355
13. Xu L, Zhou L, Li P. CIDE proteins and lipid metabolism. Arterioscler Thromb Vasc Biol 2012;32:1094–1098
14. Slayton M, Gupta A, Balakrishnan B, Puri V. CIDE proteins in human health and disease. Cells 2019;8:238
15. Sans A, Bonnafous S, Rousseau D, et al. The differential expression of Cide family members is associated with NAFLD progression from steatosis to steatohepatitis. Sci Rep 2019;9:7501
16. Aibara D, Matsuo K, Yamano S, Matsusue K. Fat-specific protein 27b is regulated by hepatic peroxisome proliferator-activated receptor γ in hepatic steatosis. Endocr J 2020;67:37–44
17. Matsusue K, Kusakabe T, Noguchi T, et al. Hepatic steatosis in leptin-deficient mice is promoted by the PPARgamma target gene Fsp27. Cell Metab 2008;7:302–311

18. Xu MJ, Cai Y, Wang H, et al. Fat-specific protein 27/CIDEC promotes development of alcoholic steatohepatitis in mice and humans. Gastroenterology 2015;149:1030–41.e6
19. Hall AM, Brunt EM, Klein S, Finck BN. Hepatic expression of cell death-inducing DFFA-like effector C in obese subjects is reduced by marked weight loss. Obesity (Silver Spring) 2010;18:417–419
20. Xu X, Park JG, So JS, Lee AH. Transcriptional activation of Fsp27 by the liver-enriched transcription factor CREBH promotes lipid droplet growth and hepatic steatosis. Hepatology 2015;61:857–869
21. Langhi C, Arias N, Rajamoorthi A, Basta J, Lee RG, Baldán Á. Therapeutic silencing of fat-specific protein 27 improves glycemic control in mouse models of obesity and insulin resistance. J Lipid Res 2017;58:81–91
22. Langhi C, Baldán Á. CIDEC/FSP27 is regulated by peroxisome proliferator-activated receptor alpha and plays a critical role in fasting- and diet-induced hepatosteatosis. Hepatology 2015;61:1227–1238
23. Rajamoorthi A, Arias N, Basta J, Lee RG, Baldán Á. Amelioration of diet-induced steatohepatitis in mice following combined therapy with ASO-Fsp27 and fenofibrate. J Lipid Res 2017;58:2127–2138
24. Kasano-Camones CI, Takizawa M, Iwasaki W, et al. Synergistic regulation of hepatic Fsp27b expression by HNF4α and CREBH. Biochem Biophys Res Commun 2020;530:432–439
25. Aibara D, Matsusue K, Takiguchi S, Gonzalez FJ, Yamano S. Fat-specific protein 27 is a novel target gene of liver X receptor α. Mol Cell Endocrinol 2018;474:48–56
26. Zhao Z, Yin L, Wu F, Tong X. Hepatic metabolic regulation by nuclear factor E4BP4. J Mol Endocrinol 2021;66:R15–R21
27. Yin J, Zhang J, Lu Q. The role of basic leucine zipper transcription factor E4BP4 in the immune system and immune-mediated diseases. Clin Immunol 2017;180:5–10
28. Tong X, Li P, Zhang D, et al. E4BP4 is an insulin-induced stabilizer of nuclear SREBP-1c and promotes SREBP-1c-mediated lipogenesis. J Lipid Res 2016;57:1219–1230
29. Matsumura T, Ohta Y, Taguchi A, et al. Liver-specific dysregulation of clock-controlled output signal impairs energy metabolism in liver and muscle. Biochem Biophys Res Commun 2021;534:415–421
30. Yang M, Zhang D, Zhao Z, et al. Hepatic E4BP4 induction promotes lipid accumulation by suppressing AMPK signaling in response to chemical or diet-induced ER stress. FASEB J 2020;34:13533–13547
31. Zheng Z, Kim H, Qiu Y, et al. CREBH couples circadian clock with hepatic lipid metabolism. Diabetes 2016;65:3369–3383
32. Flotho A, Melchior F. Sumoylation: a regulatory protein modification in health and disease. Annu Rev Biochem 2013;82:357–385
33. Gareau JR, Lima CD. The SUMO pathway: emerging mechanisms that shape specificity, conjugation and recognition. Nat Rev Mol Cell Biol 2010;11:861–871
34. Stein S, Lemos V, Xu P, et al. Impaired SUMOylation of nuclear receptor LRH-1 promotes nonalcoholic fatty liver disease. J Clin Invest 2017;127:583–592
35. Hendriks IA, D'Souza RC, Yang B, Verlaan-de Vries M, Mann M, Vertegaal AC. Uncovering global SUMOylation signaling networks in a site-specific manner. Nat Struct Mol Biol 2014;21:927–936
36. Kostrzewski T, Borg AJ, Meng Y, et al. Multiple levels of control determine how E4bp4/Nfil3 regulates NK cell development. J Immunol 2018;200:1370–1381
37. Qiu B, Simon MC. BODIPY 493/503 staining of neutral lipid droplets for microscopy and quantification by flow cytometry. Bio Protoc 2016;6:e1912
38. Bligh EG, Dyer WJ. A rapid method of total lipid extraction and purification. Can J Biochem Physiol 1959;37:911–917
39. Irizarry RA, Hobbs B, Collin F, et al. Exploration, normalization, and summaries of high density oligonucleotide array probe level data. Biostatistics 2003;4:249–264
40. Ramachandran P, Pellicoro A, Vernon MA, et al. Differential Ly-6C expression identifies the recruited macrophage phenotype, which orchestrates the regression of murine liver fibrosis. Proc Natl Acad Sci U S A 2012;109:E3186–E3195
41. Kumagai K, Tabu K, Sasaki F, et al. Glycoprotein nonmetastatic melanoma B (Gpnmb)-positive macrophages contribute to the balance between fibrosis and fibrolysis during the repair of acute liver injury in mice. PLoS One 2015;10:e0143413
42. Wang H, Zhao Y, Bradbury JA, et al. Cloning, expression, and characterization of three new mouse cytochrome p450 enzymes and partial characterization of their fatty acid oxidation activities. Mol Pharmacol 2004;65:1148–1158
43. Tanaka N, Matsubara T, Krausz KW, Patterson AD, Gonzalez FJ. Disruption of phospholipid and bile acid homeostasis in mice with nonalcoholic steatohepatitis. Hepatology 2012;56:118–129
44. Yuan Y, Zhu C, Wang Y, et al. α-Ketoglutaric acid ameliorates hyperglycemia in diabetes by inhibiting hepatic gluconeogenesis via serpina1e signaling. Sci Adv 2022;8:eabn2879
45. Wilson CG, Tran JL, Erion DM, Vera NB, Febbraio M, Weiss EJ. Hepatocyte-specific disruption of CD36 attenuates fatty liver and improves insulin sensitivity in HFD-fed mice. Endocrinology 2016;157:570–585
46. Csak T, Ganz M, Pespisa J, Kodys K, Dolganiuc A, Szabo G. Fatty acid and endotoxin activate inflammasomes in mouse hepatocytes that release danger signals to stimulate immune cells. Hepatology 2011;54:133–144
47. Cowell IG. E4BP4/NFIL3, a PAR-related bZIP factor with many roles. BioEssays 2002;24:1023–1029
48. Keniry M, Dearth RK, Persans M, Parsons R. New frontiers for the NFIL3 bZIP transcription factor in cancer, metabolism and beyond. Discoveries (Craiova) 2014;2:e15
49. Yoshitane H, Asano Y, Sagami A, et al. Functional D-box sequences reset the circadian clock and drive mRNA rhythms. Commun Biol 2019;2:300
50. Zhou L, Xu L, Ye J, et al. Cidea promotes hepatic steatosis by sensing dietary fatty acids. Hepatology 2012;56:95–107
51. Rohm M, Sommerfeld A, Strzoda D, et al. Transcriptional cofactor TBLR1 controls lipid mobilization in white adipose tissue. Cell Metab 2013;17:575–585
52. Huang X, Li Z, Hu J, et al. Knockout of Wdr1 results in cardiac hypertrophy and impaired cardiac function in adult mouse heart. Gene 2019;697:40–47
53. Liu YR, Wang JQ, Huang ZG, et al. Histone deacetylase-2: A potential regulator and therapeutic target in liver disease (review). Int J Mol Med 2021;48:131
54. Thomas T, Dixon MP, Kueh AJ, Voss AK. Mof (MYST1 or KAT8) is essential for progression of embryonic development past the blastocyst stage and required for normal chromatin architecture. Mol Cell Biol 2008;28:5093–5105
55. Lei H, denDekker AD, Li G, et al. Dysregulation of intercellular signaling by MOF deletion leads to liver injury. J Biol Chem 2021;296:100235
56. Wang M, Liu H, Zhang X, et al. Lack of Mof reduces acute liver injury by enhancing transcriptional activation of Igf1. J Cell Physiol 2021;236:6559–6570
57. Kim DH, Xiao Z, Kwon S, et al. A dysregulated acetyl/SUMO switch of FXR promotes hepatic inflammation in obesity. EMBO J 2015;34:184–199
58. Amir M, Yu M, He P, Srinivasan S. Hepatic autonomic nervous system and neurotrophic factors regulate the pathogenesis and progression of non-alcoholic fatty liver disease. Front Med (Lausanne) 2020;7:62
59. Hodson L, Gunn PJ. The regulation of hepatic fatty acid synthesis and partitioning: the effect of nutritional state. Nat Rev Endocrinol 2019;15:689–700
60. Shin DW. Lipophagy: molecular mechanisms and implications in metabolic disorders. Mol Cells 2020;43:686–693
61. Woodside WF, Ontko JA. Regulation of triglyceride mobilization in isolated hepatocytes by dibutyryl cyclic AMP and epinephrine. J Cardiovasc Pharmacol 1989;13(Suppl. 2):S38–S44; discussion S44
62. Elias JA, Tang W, Horowitz MC. Cytokine and hormonal stimulation of human osteosarcoma interleukin-11 production. Endocrinology 1995;136:489–498
63. Gómez-Lechón MJ, Donato MT, Martínez-Romero A, Jiménez N, Castell JV, O'Connor JE. A human hepatocellular in vitro model to investigate steatosis. Chem Biol Interact 2007;165:106–116
64. Filippopoulou C, Simos G, Chachami G. The role of sumoylation in the response to hypoxia: an overview. Cells 2020;9:2359

65. Jiang Z, Fan Q, Zhang Z, et al. SENP1 deficiency promotes ER stress-induced apoptosis by increasing XBP1 SUMOylation. Cell Cycle 2012;11:1118–1122
66. Hou X, Yang Z, Zhang K, Fang D, Sun F. SUMOylation represses the transcriptional activity of the unfolded protein response transducer ATF6. Biochem Biophys Res Commun 2017;494:446–451
67. Lee GY, Jang H, Lee JH, et al. PIASy-mediated sumoylation of SREBP1c regulates hepatic lipid metabolism upon fasting signaling. Mol Cell Biol 2014;34:926–938
68. Liu Y, Yu F, Han Y, et al. SUMO-specific protease 3 is a key regulator for hepatic lipid metabolism in non-alcoholic fatty liver disease. Sci Rep 2016; 6:37351
69. Wahlang B, McClain C, Barve S, Gobejishvili L. Role of cAMP and phosphodiesterase signaling in liver health and disease. Cell Signal 2018;49:105–115
70. Tao X, He H, Peng J, et al. Overexpression of PDE4D in mouse liver is sufficient to trigger NAFLD and hypertension in a CD36-TGF-β1 pathway: therapeutic role of roflumilast. Pharmacol Res 2022;175:106004
71. Tong T, Ryu SE, Min Y, et al. Olfactory receptor 10J5 responding to α-cedrene regulates hepatic steatosis via the cAMP-PKA pathway. Sci Rep 2017;7:9471
72. London E, Nesterova M, Sinaii N, et al. Differentially regulated protein kinase A (PKA) activity in adipose tissue and liver is associated with resistance to diet-induced obesity and glucose intolerance in mice that lack PKA regulatory subunit type IIα. Endocrinology 2014;155:3397–3408